Persistence of soil organic matter in eroding versus depositional landform positions

Asmeret Asefaw Berhe,[1] Jennifer W. Harden,[2] Margaret S. Torn,[3,4] Markus Kleber,[5] Sarah D. Burton,[6] and John Harte[4]

Received 22 June 2011; revised 21 February 2012; accepted 17 April 2012; published 2 June 2012.

[1] Soil organic matter (SOM) processes in dynamic landscapes are strongly influenced by soil erosion and sedimentation. We determined the contribution of physical isolation of organic matter (OM) inside aggregates, chemical interaction of OM with soil minerals, and molecular structure of SOM in controlling storage and persistence of SOM in different types of eroding and depositional landform positions. By combining density fractionation with elemental and spectroscopic analyses, we showed that SOM in depositional settings is less transformed and better preserved than SOM in eroding landform positions. However, which environmental factors exert primary control on storage and persistence of SOM depended on the nature of the landform position considered. In an annual grassland watershed, protection of SOM by physical isolation inside aggregates and chemical association of organic matter (complexation) with soil minerals, as assessed by correlation with radiocarbon concentration, were more effective in the poorly drained, lowest-lying depositional landform positions, compared to well-drained landform positions in the upper parts of the watershed. Results of this study demonstrated that processes of soil erosion and deposition are important mechanisms of long-term OM stabilization.

Citation: Berhe, A. A., J. W. Harden, M. S. Torn, M. Kleber, S. D. Burton, and J. Harte (2012), Persistence of soil organic matter in eroding versus depositional landform positions, *J. Geophys. Res.*, *117*, G02019, doi:10.1029/2011JG001790.

1. Introduction

[2] The terrestrial biosphere is dominated by sloping landscapes [*Staub and Rosenzweig*, 1986] where biogeochemical cycling of essential elements is controlled by interaction of geomorphic, pedogenic, and ecological processes that shape them. Recent studies have highlighted the important role of soil erosion in dynamics of soil organic matter (SOM) [*Berhe et al.*, 2007, 2008; *Boix-Fayos et al.*, 2009; *Harden et al.*, 1999; *Smith et al.*, 2001; *Stallard*, 1998a; *Van Oost et al.*, 2007]. However, most process level studies of SOM cycling are dominantly located on nonsloping sites that experience minimal soil erosion and deposition and thus they fail to capture the influence of topography on SOM dynamics.

1.1. Erosion-Induced Terrestrial Carbon Sequestration

[3] Annually, water erosion is estimated to move 30–100 Pg soil and 1–5 Pg carbon (C) globally—70 to 90% of which is deposited within the same or adjacent watersheds [*McCarty and Ritchie*, 2002; *Stallard*, 1998b; *Starr et al.*, 2001]. It has been shown that erosion and terrestrial deposition can act as a C sink for the atmosphere with an estimated strength of up to 1.5 Pg C yr^{-1} [*Berhe et al.*, 2007; *Harden et al.*, 1999; *Stallard*, 1998b; *Van Oost et al.*, 2007]. Soil erosion constitutes a C sink if posterosion watershed C stocks increase due to replacement of eroded C by production of new photosynthate at eroding positions and/or reduced decomposition rate of at least some of the eroded C in depositional landform positions [*Berhe et al.*, 2007].

[4] Studies on the role of soil erosion in terrestrial C sequestration typically focus on quantifying changes in the inventory of C in eroding watersheds over time [*Quine and Van Oost*, 2007; *Smith et al.*, 2001; *Stallard*, 1998a; *Van Oost et al.*, 2005, 2007]. Except in a few studies [*Berhe et al.*, 2008; *Billings et al.*, 2010; *Harden et al.*, 1999; *Nadeu et al.*, 2011], stability and stabilization mechanisms of SOM have not been addressed in the context of the erosion-induced terrestrial C sequestration. Hence we lack a good understanding of which mechanisms of SOM stabilization are most important during detachment of aggregates by rain splash, transport of eroded particles downslope, or decomposition postdeposition.

[1]School of Natural Sciences, University of California, Merced, Atwater, California, USA.
[2]Geologic Division, U.S. Geological Survey, Menlo Park, California, USA.
[3]Earth Sciences Division, Lawrence Berkeley National Laboratory, Berkeley, California, USA.
[4]Energy and Resources Group, University of California, Berkeley, California, USA.
[5]Department of Crop and Soil Science, Oregon State University, Corvallis, Oregon, USA.
[6]Environmental Molecular Science Laboratory, Pacific Northwest National Laboratory, Richland, Washington, USA.

Corresponding author: A. A. Berhe, School of Natural Sciences, University of California, Merced, 4225 N. Hospital Rd., Atwater, CA 95301, USA. (aaberhe@ucmerced.edu)

0148-0227/12/2011JG001790

1.2. Mechanisms of Soil Organic Carbon Stabilization in the Context of Erosion and Sedimentation

[5] In this study, we adopt the definition of stability of SOM as its persistence in the soil system [*Schmidt et al.*, 2011]. In eroding watersheds that experience lateral redistribution of topsoil by soil erosion, stability of SOM (as inferred from MRT or ^{14}C, for example) does not necessary indicate time spent in a specific profile, at a specific landform position, rather it is more accurate when used to indicate time spent in the whole watershed.

[6] Three mechanisms had been previously recognized as governing stabilization of SOM: physical isolation of SOM inside aggregates, chemical interaction of OM with the soil matrix, and molecular composition of SOM [*Christensen*, 1992; *Sollins et al.*, 1996; *Stevenson*, 1994]. Recently, the importance of molecular composition (also referred to as recalcitrance) as an important factor for SOM persistence has been challenged [*Kleber*, 2010b; *Schmidt et al.*, 2011]. Here, we provide a brief discussion on how physical isolation, chemical interaction, and molecular structure of SOM are related to dynamics of SOM in eroding watersheds.

1.2.1. Physical Isolation of SOM

[7] In both eroding and depositional positions of a given watershed, SOM can be protected from decomposition by physical isolation of OM inside aggregates of soil particles and/or burial in deep soil layers. Aggregation can render organic compounds physically inaccessible to soil microbes and fauna, and restrict the rate of diffusion of oxygen and enzymes [*Kleber*, 2010b; *Sexstone et al.*, 1985; *Six et al.*, 2002; *Sollins et al.*, 1996]. In a similar manner, burial of topsoil material in subsoils of depositional positions could slow down decomposition by changing the environmental drivers of SOM decomposition, such as by reducing O_2 availability and/or changing soil moisture content [*Berhe*, 2012].

[8] Redistribution of SOM with soil erosion can both increase and decrease accessibility of SOM to decomposition. Early in the redistribution process, protective macroaggregates are broken down and finer mineral soil particles and light organic particles are suspended (in the case of water erosion), increasing the probability that previously physically protected SOM will be accessed by decomposer organisms and enzymes. Breakdown of aggregates also facilitates oxygenation and hydration of the previously enclosed OM, further enhancing the potential for its decomposition. However, after deposition, burial in depositional soil profiles with high bulk density, low total porosity, and small pore sizes impedes access by decomposers and their enzymes, and hinders the diffusion of oxygen and moisture. Moreover, redistribution can also put OM in a new *matrix context*, where an organic fragment that was previously surrounded by large sand grains may be deposited among silt and/or clay particles thus allowing the formation of tighter and more efficient physical barriers for decomposition. The net effect of redistribution on OM decomposition will depend on the duration of the exposure and transport phases; depth of burial, and the type of newly created matrix context.

1.2.2. Interaction With Soil Minerals

[9] In aerobic soils, the oldest SOC tends to be associated with soils that have high clay content, high concentration of aluminum (Al) and iron (Fe) oxy(hydr)oxides, large specific surface area (SSA, externally available sorption sites), and high sum of exchangeable cations (as indicated by cation exchange capacity, CEC) [*Kahle et al.*, 2002; *Kaiser and Guggenberger*, 2001; *Masiello et al.*, 2004; *Mayer and Xing*, 2001; *Mikutta et al.*, 2006; *Oades*, 1988]. Thus considerable SOC storage and stabilization is associated with organo-mineral complexation phenomena controlled by soil mineralogy and pedogenesis [*Eusterhues et al.*, 2003]. Decomposition may be retarded by chelation of organic acids with Fe^{3+} and Al^{3+} to form metastable intermediate organo-metal complexes [*Boudot*, 1992; *Masiello et al.*, 2004; *Oades*, 1995; *Rasmussen et al.*, 2005; *Tate*, 1992; *Torn et al.*, 1997] or by interactions with poorly crystalline or amorphous minerals such as ferrihydrite. These metastable oxyhydroxides are characterized by high specific surface area, variable charge, high degree of hydration, and are capable of forming OM-mineral bonds through innersphere ligand exchange reactions [*Masiello et al.*, 2004] as well as adsorb anions by a combination of electrostatic attraction and surface complexation [*Masiello et al.*, 2004; *Oades*, 1988; *Torn et al.*, 1997].

[10] Erosion can bring dissolved OM and/or previously unprotected particulate OM into contact with mineral surfaces and enable sorptive protection. Upon deposition, eroded OM enters a new matrix context where the finer soils particles, including reactive colloids that are preferentially transported by water erosion, are deposited. This chemical mechanism of SOM stabilization should be most effective if erosion removes OM from an area that has relatively higher concentration of unreactive (such as low-charge siloxane) mineral surfaces and deposits it in environments with relatively higher abundance of more reactive minerals (such as hydroxylated Fe oxides). Sorption of OM on surfaces of Fe oxides can lead to formation of innersphere complex bonds that provide increased protection against desorption of OM from mineral surfaces.

1.2.3. Molecular Structure

[11] SOM comprises a collection of simple and macromolecular organic functional groups [*Krull et al.*, 2003; *Sollins et al.*, 1996]. The mean residence times (MRT) of different compounds can vary widely depending on their association with the soil matrix and environmental conditions. By changing the physical, biological, and microclimatic conditions in environments where a given SOM pool or compound class resides, transport and deposition can change its decomposition rate, and some types of SOM might be expected to be more strongly influenced by the change in environment [*Berhe et al.*, 2007; *Schmidt et al.*, 2011; *Trumbore*, 2009]. For example, let's consider a case where SOM from slopes is laterally transported by soil erosion to an environment that is waterlogged, as is the case in valley floors or depositional positions such as our plain position that is waterlogged for at least for part of the year. Lateral redistribution with soil erosion can lead to transfer of OM from well aerated soil profiles at slopes to depositional environments that are waterlogged, less oxygenated, have lower density of active microbes—where the conditions in the depositional valley floor or plain are less optimal for decomposition. In theory, in the short term this could lead to reduced decomposition of organic compounds that are less soluble, larger, and have high stoichiometric oxygen demand (for decomposition) than others. But, these short-term dynamics should not be confused with long-term resistance of organic functional groups to decomposition. Molecular structure alone does not control long-term

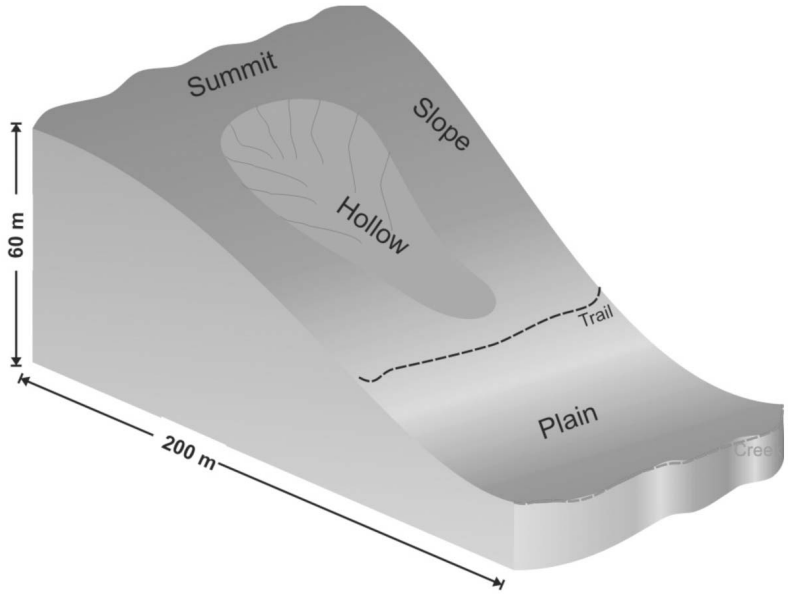

Figure 1. Schematic representation of study site (not to scale) along with the sampling locations within the watershed.

decomposition dynamics of SOM [*Kleber*, 2010a, 2010b; *Schmidt et al.*, 2011].

1.3. Objectives and Hypotheses

[12] The objective of this study was to characterize the relative importance of different mechanisms that may extend the residence time of SOM in eroding versus depositional landform positions. We hypothesized that (1) physical stabilization (aggregate protection) of SOM is more important in depositional landform positions, represented by hollow and plain in this study, compared to the eroding positions; (2) chemical stabilization of SOM (sorptive protection against decomposition by soil minerals) is more important in depositional, compared to eroding landform positions; and (3) there is less change in SOM composition with soil depth in the depositional landform positions, compared to eroding positions. We studied an annual grassland watershed in California with four types of landform positions: summit, slope, hollow, and plain. As we investigate whether SOM is stored effectively in depositional versus eroding positions, we expected the residence time of soil mineral particles to be longer in depositional compared to eroding landform positions. We evaluate the effectiveness of different landform positions for SOM storage by (1) computing the weighted average ^{14}C content of each profile, (2) determining if more C is stored inside aggregates in the depositional versus eroding landform positions, (3) correlating the stock of bulk SOM and fraction of OM in the dense fraction (DF) with Fe and Al oxides, and (4) determining the distribution of SOM functional groups and ratio of alkyl to O-alkyl groups in SOM at the different landform positions.

2. Methods

2.1. Study Site

[13] This study was carried out at Tennessee Valley (TV) in Marin County, northern California. A geomorphic, edaphic, and vegetation description of our study site was previously provided in *Berhe et al.* [2008]. Briefly, the climate at TV is Mediterranean, with mean annual temperature of 14°C and mean annual precipitation of 1,200 mm. The dominant vegetation cover includes Mediterranean annual grasses and a coastal shrub (*Baccharis pilularis*) that is recently encroaching onto the summit, slope and hollow. The study site is protected within the Golden Gate National Recreation Area (GGNRA), and has not been subjected to any documented anthropogenic disturbance since 1972 [*Heimsath et al.*, 1999].

2.2. Soil Properties

[14] Soils at TV are derived from chert, greenstone, and Franciscan sandstone parent material. Soils in the eroding slopes are classified as Lithic Haplustolls while those on the foot slopes are classified as Lithic Ustorthents and those on the depositional profiles are classified as Oxyaquic Haplustolls [*Yoo*, 2003]. The rate of soil erosion ranges from 50 to 130 g m^{-2} yr^{-1}, and the corresponding SOC erosion is around 2 g m^{-2} yr^{-1} [*Heimsath et al.*, 1999; *Yoo et al.*, 2005].

[15] We dug pits and collected soil samples from four geomorphically distinct landform positions: two eroding (the summit, and the back slope, or slope) and two depositional (a depressional hollow and an alluvial/colluvial plain) (Figure 1). We collected samples from six soil profiles in the summit, eight in the slope, six in the hollow, and seven in the plain. From each profile, soil samples were collected at depth increments of 0–5 cm, 5–15 cm, then every 15 cm down to 120 cm, and finally every 30 cm until the soil-saprolite boundary. Soil pH was measured in a 1:1 soil: water slurry, bulk density was determined by a combination of core and clod/ped methods [*Blake and Hartge*, 1986], and particle size distribution was determined using the hydrometer method [*Sheldrick and Wang*, 1993]. Cation exchange capacity (CEC) was determined using the barium acetate, calcium replacement technique [*Janitzky*, 1986]. Specific

surface area (SSA) measurements were performed with N_2 gas adsorption at 77 K using a Micrometrics, Tristar 3000 automated gas adsorption analyzer (Micrometrics Instrument Corporation, Norcross, GA) and SSA calculated using the Brunauer-Emmett-Teller (BET) equation [*Brunauer et al.*, 1938].

2.2.1. Carbon and Nitrogen

[16] For elemental and isotopic measurements of C and nitrogen (N), the samples were air dried, sieved to <2 mm, and ground using mortar and pestle to pass through a 100 mesh sieve. Percent C and N were measured with a Carlo Erba elemental analyzer, while the $\delta^{13}C$ was measured using a PDZ Europa Scientific 20/20 Mass Spectrometer and referenced to the Pee Dee Belemnite standard. Similarly, harvested plant matter (extensive description of the sampling methodology of foliage is given in *Berhe* [2012]) was oven dried at 60°C for 48 h and ground with a Spex mill, and then with a Wig-L-bug mill until all fibrous material disappeared before it was analyzed for C, N, and $\delta^{13}C$ composition. Analytical precision, determined as the standard deviation obtained by repeated combustions of the same homogenized sample, was 0.05% N and 0.05% C for the Carlo Erba, and 0.13‰ δ^{13} C for the Europa mass spectrometer.

[17] The C inventory for the entire depth profile was calculated as

$$C_{\text{inv}} = \sum \Delta Z \cdot \rho_i \cdot (1 - R_i) \cdot (\%OC \cdot 100) \quad (1)$$

where C_{inv} (g C/m^2) is carbon inventory over the entire depth profile, ΔZ_i (cm) is thickness of ith soil layer, ρ_i = bulk density (g/cm^3), R_i is rock fraction, and $\%C$ is organic C concentration in the <2 mm fraction of soil in each layer. The samples were not pretreated with acid for carbonate removal prior to C analysis because the inorganic C content of the soils is negligible [*Yoo*, 2003].

[18] The radiocarbon content of bulk SOM for all sampled soil layers and respective SOM fractions from one profile in each of the landform positions was analyzed at the W. M. Keck Carbon Cycle Accelerator Mass Spectrometry (AMS) Laboratory. Graphite was prepared by sealed tube Zn reduction following the methods of *Trumbore et al.* [1989] and *Vogel* [1992]. The estimated precision of graphitization and AMS measurement on modern samples at the Keck AMS is about 2–3 ‰ based on long-term duplicate analyses of standards and samples [*Khosh et al.*, 2010; *Xu et al.*, 2007]. ^{14}C content is expressed as fraction modern (FM) or $\Delta^{14}C$ [*Stuiver and Polach*, 1977].

[19] We compare C storage effectiveness at the different locations on the watershed using C-weighted average FM value, FM_w. A site is said to be effective in C storage if, for the same rate of input, it retains bigger stock of old C (that has more negative $\Delta^{14}C$). A site that is effective in C storage would have small FM_w values (~0) because it would have retained relatively more old C. The opposite is true for a site that is less effective in C storage and would have FM_w values closer to 1. The FM_w for one profile from each position (summit, slope, hollow, and plain) was calculated according to the methods of *Torn et al.* [1997] and *Masiello et al.* [2004] as:

$$FM_w = \frac{1}{C_{inv,tt}} \cdot \sum FM_i \cdot C_{inv,i} \quad (2)$$

where $C_{inv,tt}$ is the C_{inv} derived for each profile in equation (1) (tt = total), FM_i is FM value of the C in each layer and $C_{inv,i}$ is C_{inv} for the *ith* layer.

2.2.2. Density Fractionation

[20] The bulk soil was separated into three density fractions—free light fraction (fLF), occluded light fraction (oLF), and dense fraction (DF)—using 1.7 g cm^{-3} sodium polytungstate [SPT, $Na_6(H_2W_{12}O_{40})$] solution according to the methods of *Swanston et al.* [2005], *Strickland and Sollins* [1987], and *Golchin et al.* [1994]. Briefly, a 20 g soil sample was placed in a centrifuge bottle with 75 ml of SPT, and inverted gently (by hand) five times, let to settle undisturbed for 45 min, and centrifuged at 3500 rpm for 1 h. The fLF, which consists mainly of partly decomposed plant fragments, was removed by aspirating floating material into a sidearm flask. To extract the oLF, the remaining soil mixture was mixed for 1 min with 75 mL SPT using a desktop mixer, sonicated for 3 min at 70% pulse, and centrifuged at 3500 rpm for 1 h according to the methods of *Swanston et al.* [2005]. Preliminary tests that included sonication and wet sieving were used to determine that the applied ultrasonic energy level was sufficient to disperse all aggregates greater than 53 μm in two representative samples. Materials floating on the supernatant were aspirated into a sidearm flask. The extracted fLF and oLF were separately rinsed five times with deionized water, filtered to pass through a 0.8 μm membrane filter, after which the filtrate was discarded and the residue oven dried for 24–48 h. The residue was rinsed five times with 150 mL double-deionized (MilliQ) water to remove the SPT, followed by centrifugation for 20 min to 1 h. Finally, the DF was oven dried for 24–48 h.

[21] Analytical precision, as determined by the standard deviation of repeated fractionation of the same sample (test carried out with 10 individual samples), was 2.04% for the recovery efficiency, 0.04% of total mass for the fLF, 0.11% of total mass for the oLF and 0.11% of total mass for the DF. In this procedure, it wasn't possible to determine which fraction the C lost during the fractionation steps would have been derived from. For the purpose of calculating distribution of recovered C in the different fractions (fLF, oLF or DF), we assumed that the recovered mass is equivalent to total mass.

2.2.3. Selective Dissolutions

[22] Three selective dissolutions for Fe and Al oxides, hydroxides and oxyhydroxides (of the form MO_x, $M(OH)_x$, or MO_xOH_x respectively, where M = metal (Fe and Al)) were performed to determine the stock of three classes of mineral functional groups that can chemically protect SOM from decomposition–crystalline Fe, poorly crystalline Fe and Al oxides, and chelated organo-metal complexes. The concentration of crystalline primary Fe oxides plus non-crystalline Fe oxyhydroxides was determined using citrate-dithionite with one 16 h extraction at 23°C [*McKeague*, 1967; *Torn et al.*, 1997]. The amount of poorly crystalline aluminosilicates, Fe hydroxides and organically complexed Fe and Al was measured by extraction with acid-ammonium-oxalate, with one 4 h extraction at pH 3 in the dark [*McKeague and Day*, 1966]. The proportion of organically complexed Fe and Al was estimated by sodium pyrophosphate extraction [*Loeppert and Inskeep*, 1996]. After each of these extraction procedures, the solutions were centrifuged and the supernatant filtered with a cellulose acetate 0.2 μm

filter prior to analyses for Fe and Al by ICP [*Ross and Wang*, 1993].

[23] The proportion of chelated organics associated with Fe and Al was approximated directly from the pyrophosphate extraction. The proportions of crystalline Fe and poorly crystalline Fe and Al oxides were approximated by the difference between the dithionite and oxalate extractable ions ($Fe_{d\text{-}ox}$), and by the difference between oxalate and pyrophosphate extractable Fe and Al ions ($M_{ox\text{-}py}$), respectively, while proportion of chelated organo-mineral complexes is given by pyrophosphate extractable Fe and Al (M_{py}) [*Masiello et al.*, 2004]. The inventory of metal ions extracted by the three dissolutions was calculated using an equation analogous to equation (1).

[24] Analytical precision, as determined by the standard deviation of repeated measurements on the same sample, was 0.001 g cm^{-2} for Al_{ox}, Al_{py} and Fe_{py}; and 0.003 g cm^{-2} for Fe_d and Fe_{ox}. After Gaussian error propagation for simple sums and differences, the standard deviations for analytical precision of the values of interest were 0.001 g cm^{-2} $Al_{ox\text{-}py}$, 0.002 g cm^{-2} M_{py}, 0.003 g cm^{-2} $Fe_{ox\text{-}py}$, 0.004 g cm^{-2} $Fe_{d\text{-}ox}$, and 0.004 g cm^{-2} for $M_{ox\text{-}py}$.

2.2.4. Solid-State ^{13}C Nuclear Magnetic Resonance

[25] The ^{13}C NMR spectra of foliage from two types of vegetation, *B. pilularis* shrub, and annual grasses, growing in different parts of our study watershed were first determined to compare biochemical composition of the inputs of SOM into the eroding and depositional landform positions. For soils, prior to nuclear magnetic resonance (NMR) spectroscopy, the dense fraction (DF) and bulk soils were treated with hydrofluoric acid (HF) to decrease the amount of paramagnetic materials (especially Fe^{3+} and Mn) that interfere with the NMR signal and to concentrate OM in the sample according to the methods of *Eusterhues et al.* [2003]. The amount of organic C lost in the procedure was calculated by simple mass balance [*Schmidt and Gleixner*, 2005]. According to *Schmidt et al.* [1997], this HF demineralization procedure does not cause significant changes in SOM composition, but may result in some loss of carbohydrates. The ^{13}C NMR spectra of the HF demineralized bulk and DF samples then represent molecular Structure of the fraction that survives the acidic extraction, and not that of the total SOM content.

[26] The solid-state ^{13}C nuclear magnetic resonance (NMR) spectra were obtained from a Varian Infinity CMX 300 MHz spectrometer at the William R. Wiley Environmental Molecular Sciences Laboratory, Pacific Northwest National Laboratory. Each sample was packed in a 5 mm zirconia rotor, fitted with boron-nitrite spacers and KEL-F (low carbon) caps. A ramped (^{13}C pulse) cross polarization magic angle spinning (CPMAS) pulse sequence was used. The contact time was 1 ms, the spinning rate was 10 kHz, and the decoupling field was 63–55 kHz. The ^{13}C chemical shifts were referenced to tetramethylsilane (0 ppm) using an external reference, hexametabenzene (HMB) (16.81 ppm). We took 3000 scans for plant samples, 12,000 scans for the free light and occluded light fractions and up to 100,000 scans for hydrogen fluoride (HF) demineralized bulk soils and >1.7 g cm^{-3} DF. After Fourier transformation, we applied line broadening of 200 Hz for all samples.

[27] Molecular composition is inferred by dividing the ^{13}C NMR spectra into four chemical shift regions that correspond to four functional groups alkyls (0–45 ppm), O-alkyls (45–110 ppm), aromatic (110–160 ppm), and carboxyl C (160–220 ppm) [*Baldock et al.*, 1992, 1997]. The proportion of C in each functional group was computed by integrating the area under the individual peaks of the functional group region [*Swift*, 1996]. We used the relative difference of the peaks [alkyl to O-alkyl ratio (A:O-A)] as a measure of the degree of decomposition of organic compounds in soils [*Baldock et al.*, 1997]. The fraction of aromatic functional groups in total OM (aromaticity index) was calculated by integrating areas under aliphatic and aromatic peaks such that aromaticity = $[(110 - 160)/(0 - 160)]$. In this computation, the area under the carboxyl peak (160–220 ppm) is not included because it can be assigned to both straight chain and aromatic C structures [*Rovira and Vallejo*, 2002]. All spectra processing was performed using MestReC software (version 4.59, Universidad de Santiago de Compostela, Spain).

2.3. Data Analysis

[28] All data are expressed as means with standard error of variables. Location means were compared using the Wilcoxon/Kruskal-Wallis nonparametric tests for means comparisons. We used a least squares nested ANOVA test for main effects of depth (nested in each landform position) and landform position on separation of OM into different density fractions in our study toposequence. Pairs of means at the different depths and landform positions were also compared using the Tukey-Kramer HSD test, and simple linear regression was used to assess the proportion of variability in SOM storage and stability that is accounted for by different properties of the soil mineral fraction. For all statistical tests, a significance level of $p < 0.05$ was set before hand as the α level. All statistical tests were performed using JMP 6.0.0 software (SAS, Cary, NC).

3. Results

[29] Soils at the different landform positions differed in their physical and chemical properties. The pH of soil samples in the hollow was slightly acidic (5.5–6.5 pH in water), whereas the soils in the summit, slope, and plain profiles ranged from slightly acidic (pH 5.4–6 in water) to neutral (pH 6.5–7.2 pH water; see Table 1). At comparable depths, the plain had significantly higher clay content (profile average of 43%) compared to the other three landform positions (27%). Bulk density (BD, g cm^{-3}) increased as a function of depth (z, cm) with fairly similar linear regression parameters for all sites: ($BD = 0.01z + 1.27$, $R^2 = 0.89$ for summit; $BD = 0.03z + 1.53$, $R^2 = 0.61$ for slope, $BD = 0.04z + 1.49$, $R^2 = 0.95$ for hollow; and $BD = 0.03z + 1.68$, $R^2 = 0.81$ for plain) (see Table S1 in Text S1 of the auxiliary material for data on a comprehensive list of physicochemical properties of the soils at the different landform positions).[1]

[30] Topsoil C concentration in the <2 mm soil fraction was higher in the summit and plain profiles, compared to the other landform positions. %C in the summit showed a sharp decline with depth while %C in the plain remained high throughout the profile (Figure 2). The inventory of C was highest in the plain, with both depositional positions having

[1]Auxiliary materials are available in the HTML. doi:10.1029/2011JG001790.

Table 1. Location and Average Values for pH and Clay Content[a]

Location	Meters Above Sea Level	Sampled Depth (cm)	pH in Water	Clay (%)
Summit	105	0–5	5.9	25.8 ± 0.11
		5–15	5.6	29.8 ± 0.12
		15–30	5.6	30.7 ± 0.13
		30–45	5.9	34.7 ± 0.15
		45–69	6.6	32.7 ± 0.14
Slope	80 back slope	0–5	5.4	22.5 ± 0.87
	50 foot slope	5–15	5.4	22.3 ± 1.31
		15–30	5.8	25 ± 0.41
		30–45	6.5	25.3 ± 1.93
		45–60	6.9	28.3 ± 3.25
		60–75	6.7	25.7 ± 2.47
		75–90	6.7	28±n/a
Hollow	55–80	0–5	5.5	23.7 ± 0.76
		5–15	5.5	24.7 ± 0.29
		15–30	6.0	26 ± 0.50
		30–45	6.0	30 ± 2.29
		45–60	6.2	30.3 ± 3.06
		60–75	6.0	30 ± 3.61
		75–90	6.0	26 ± 2.12
		90–120	6.4	26 ± 2.83
		120–141	6.5	21±n/a
Plain	45	0–5	6.0	33.6 ± 1.80
		5–15	6.0	36.6 ± 0.63
		15–30	6.1	38.8 ± 0.85
		30–45	6.4	44 ± 1.08
		45–60	6.9	45.5 ± 1.55
		60–75	6.9	46.5 ± 1.04
		75–90	6.9	45.5 ± 3.01
		90–105	7.2	44.3 ± 2.78
		105–120	7.2	44 ± 4.95
		120–150	6.9	48±N/a

[a]Bottom depth represents the deepest layer of all the sampled profiles. The error term represents standard error for n = 3 in summit, n = 4 in slope, n = 3 in hollow, and n = 4 in plain. Analytical precision, determined as the standard deviation obtained by repeated measurements from the same homogenized sample, was 1% for clay.

significantly higher C_{inv} than the two eroding landform positions. In addition, the two depositional positions were also more effective at C storage than the two eroding positions (as determined from the average inventory of weighted FM in the two eroding versus the two depositional positions) (Figure 3). Bulk soil C:N ratio decreased with depth in all landform positions, except the plain. OM in the topsoil layers at the plain had the most positive $\Delta^{14}C$ of +70‰ while SOM immediately above the soil-saprolite boundary at the hollow had the most negative $\Delta^{14}C$ of −501‰ (Figure 2).

3.1. Physical Isolation of SOM

[31] Across landform positions, the C concentration of fLF—unprotected OM that contains plant fragments—was highest in the plain especially at depth, and lowest in the hollow. The fLF made up about 2.98–3.75% of total C in all the landform positions. The C:N ratio of fLF increased with depth in all landform positions, except summit. The fLF in the plain had the most positive $\Delta^{14}C$ of +92‰ of fLF in all landform positions, while fLF immediately above the soil-saprolite boundary at the summit had the most negative $\Delta^{14}C$ of −402‰ (Figure 2; Table S1 in Text S1). In 4 out of 6 layers below 50 cm, the fLF had more positive $\Delta^{14}C$ than did oLF and DF at the same depths (Figure 2). The variation in fraction of C found as fLF in each soil layer explains a significant fraction of the bulk SOC concentration and radiocarbon content at the slope and hollow at the sampled soil layers, but not the summit or plain.

[32] On average, more C was associated with oLF—the intra-aggregate fraction that was typically dark, fine organic matter rich material—in the plain, compared to all other landform positions. The oLF accounted for about 10% of total C in the plain compared to about 6% in the other landform positions (Figure 2; Table S2 in Text S1). However, the depth profiles of oLF C show considerable variability likely due to bioturbation and sedimentation from episodic, pulse-driven erosive events. In the summit, up to 8 more times C was associated with the oLF in the subsoil layers compared to topsoil. In contrast, up to 3 more times C was associated with the oLF in the subsoil versus shallower depths at the other landform positions (Figure 2). The $\Delta^{14}C$ of OM in the oLF was more negative than $\Delta^{14}C$ of the other fractions at the same depth below 25 cm in the summit and at all but one depth in the slope. In the depositional landform positions, $\Delta^{14}C$ of the OM in the oLF was more negative than the other fractions at the same depth at two soil layers below 80 cm at the hollow, and at five of the nine depths below 5 cm that we analyzed in the plain (Figure 2). The fraction of C found as oLF in each soil layer explains a significant fraction of the variability in bulk SOC stock at the different layers at the hollow and radiocarbon content at the slope, but not the other landform positions (Table 2; Table S4 in Text S1).

3.2. Interaction of SOM With Soil Minerals

[33] A larger proportion of soil C was found in the dense, mineral-associated fraction—up to 80% in the eroding and 60% in the depositional landform positions (Figure 2). The C:N ratio of DF had a narrow range, between 9 and 11, in all landform positions. The DF in the plain had the most positive $\Delta^{14}C$ of +62‰ while DF immediately above the soil-saprolite boundary at the hollow had the most negative $\Delta^{14}C$ of −526‰.

[34] CEC did not change considerably with depth or landform position. It ranged between 21 and 32 meq/100 g soil in the eroding landform positions and 21–41 meq/100 g in the depositional landform positions. CEC accounted for 86% of the variability in bulk C in the summit, but had week association with SOM concentration or radiocarbon content in any of the other landform positions (Tables S1 and S3 in Text S1). Based on simple linear regression, SSA explains more of the variability in bulk and mineral-associated C storage and radiocarbon content across depths in all landform positions than any other single variable we evaluated. Of the four landform positions, the plain profile had the lowest SSA in the topsoil and highest SSA at the bottom of the soil profile (Table S1 in Text S1).

[35] In all landform positions, the concentrations of crystalline Fe (Fe_d), and poorly crystalline Fe and Al oxides ($Fe_{ox\text{-}py}$ and $Al_{ox\text{-}py}$) were lowest at the surface and increased with depth. The concentration of Fe_{py} and Al_{py} increased until about 25cm and remained about the same or slightly decreased with depth in all landform positions, except in the hollow where Fe_{py} and Al_{py} concentrations peaked at about 100 cm depth. On average, the concentration of organo-mineral complexes as indicated by Fe_{py} and Al_{py} was higher at the depositional landform positions, compared to eroding ones ($p = 0.01$ for Fe_{py} and, $p = 0.03$ for Al_{py}). The

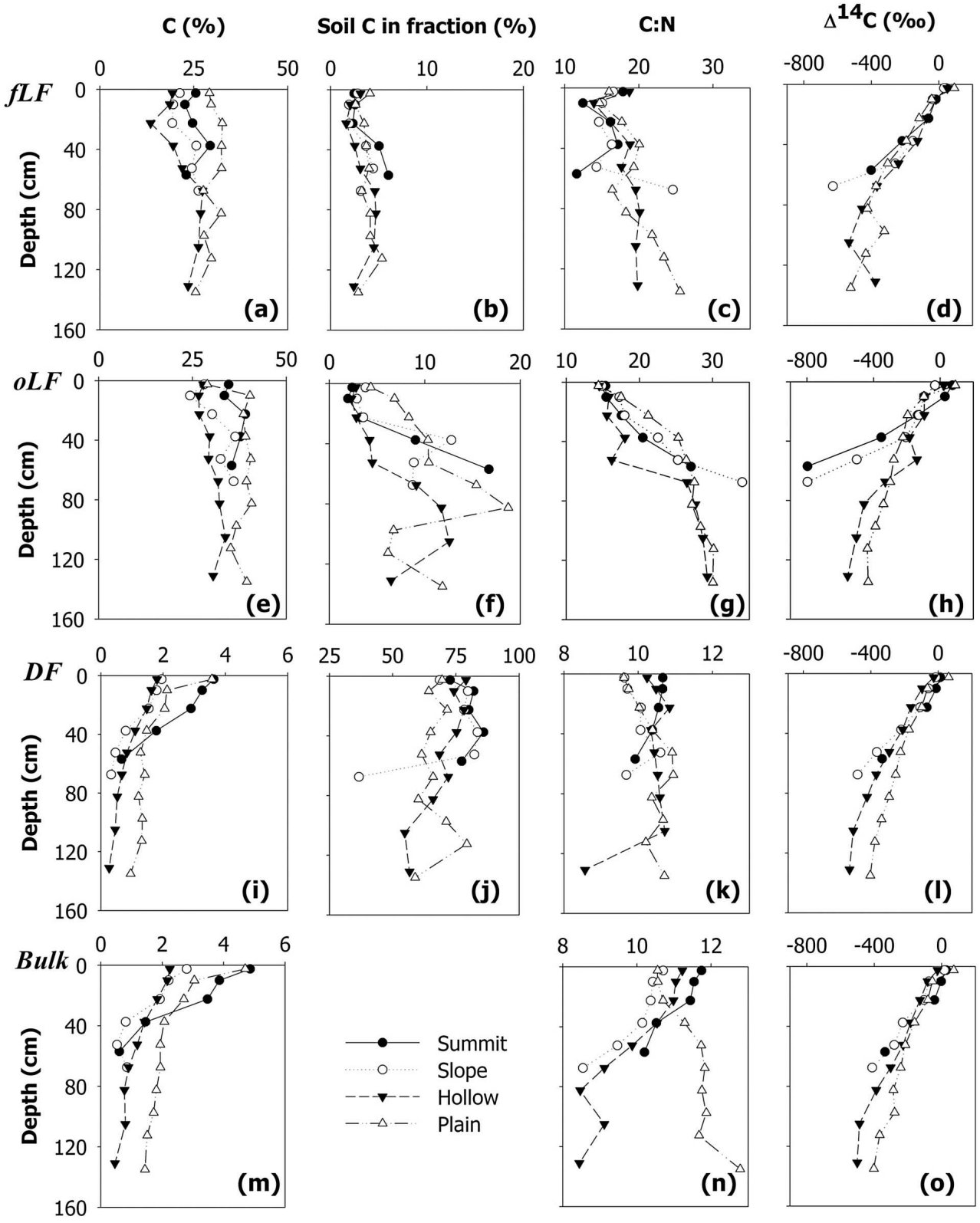

Figure 2. Average percent C and distribution of C, C:N, and $\Delta^{14}C$ of SOM in (a–d) fLF, (e–h) oLF, (i–l) DF, and (m–o) bulk soil. For $\Delta^{14}C$ of fractions, n = 1. For percent C and C:N, n = 3 in summit, n = 4 in slope, n = 3 in hollow, and n = 4 in plain. Note the different axis scales.

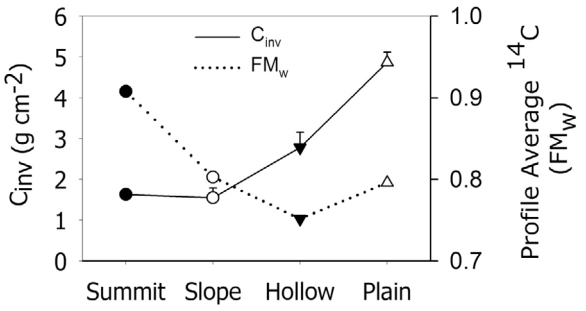

Figure 3. Inventory of C and weighted FM in the eroding and depositional profiles. Error bars for C_{inv} represent standard errors for n = 3 in the summit and hollow and for n = 4 in the slope and plain.

difference in crystalline Fe inventory between the four landform positions was statistically significant (p = 0.01). The mid slope positions of slope and hollow were zones of depletion for poorly crystalline minerals, especially $Al_{ox\text{-}py}$. The differences between the means of $Fe_{ox\text{-}py}$ (p = 0.02) and $Al_{ox\text{-}py}$ (p = 0.01) in the different landform positions were statistically significant (Figure 4).

3.3. Molecular Composition From ^{13}C NMR

3.3.1. Foliage

[36] The ^{13}C NMR spectra of both *B. pilularis* and the grasses had intense signals in the O-alkyl region around 72 ppm that are attributed to carbohydrates. *B. pilularis* (shrub) had a fairly pronounced, broad signal in the alkyl region, around 15–50 ppm, while the grasses had a discernable peak around 100 ppm, typical of methylene groups in alkyl chains and carbohydrates, respectively. The small peak around 175 ppm in the *B. pilularis* ^{13}C NMR spectra is typical of carboxyl groups (see Figure 1 in Text S1).

[37] The alkyl to O-alkyl (A:O-A) ratio of *B. pilularis* ranged from 0.46−0.59 while the A:O-A ratio of the grasses was between 0.08 and 0.1. Fraction aromaticity of *B. pilularis* ranged from 0.14 to 0.17 while that of annual grasses was 0.09–0.13 (Table S7 in Text S1). Consequently, from this point on, we assume that the same type of plants growing in different parts of the toposequence have the same starting material for SOM. The important differences in SOM input were due to the relative coverage of each vegetation type in a given landform position and differences in productivity (NPP). More information on plant distribution was given in *Berhe* [2012] and *Berhe et al.* [2008].

3.3.2. Bulk Soil Organic Matter

[38] HF demineralization of soil samples prior to NMR work, although useful, has some effects that must be noted. In our samples, the average mass recovery after HF treatment was 33% for the bulk soil samples and 32% for the DF. The HF treatment removed up to 30% and 40% of the C from sub soils of the eroding and depositional profiles, respectively (Table S6 in Text S1). The loss of C from the two eroding slope profiles reduced the resolution of the ^{13}C CPMAS NMR spectra and complicated the interpretation of the spectra for SOM below 30 cm. Specifically, after subtracting the background spectra (empty rotor with spacers and caps), the ^{13}C NMR spectra of bulk SOM at 30–45 cm and the deepest layers of summit and the slope profiles were too noisy to interpret in a meaningful way. We restrict our discussions and conclusions to the top 15 cm of bulk SOM and 45 cm of the DF spectra from the eroding slope profiles.

[39] The ^{13}C NMR spectra of bulk SOM at the surface were very similar at all four sites, but had important differences with depth. The signal intensities of the alkyl and O-alkyl peaks decreased, while intensities of the aromatic and carboxyl peaks increased with depth at all sites (Figure 5). When going from the surface layer (0–5 cm) to 5–15 cm depth, the A:O-A ratio increased in both eroding

Table 2. R^2 Values Derived From Simple Linear Regression of Bulk (Total) C Concentration, Fraction of C Associated With the DF, and Radiocarbon Content of Bulk and DF C[a]

	Bulk C				DF C				Δ^{14}C of Bulk C				Δ^{14}C of DF C			
	Summit	Slope	Hollow	Plain	Summit	Slope	Hollow	Plain	Summit	Slope	Hollow	Plain	Summit	Slope	Hollow	Plain
Bulk C	-	-	-	-	0.98	0.85	0.86	0.89	0.96	0.93	0.90	0.88	0.95	0.93	0.94	0.89
fLF C		0.37	0.32		0.47	0.49					0.47				0.45	
oLF C			0.29				0.22			0.67						
DF C	0.98	0.85	0.86	0.89	-	-	-	-	0.93		0.62	0.89	0.87	0.54	0.62	0.90
Bulk C:N	0.83	0.71	0.69	0.53	0.84	0.63	0.54	0.55	0.99	0.87	0.88	0.83	0.97	0.90	0.90	0.83
fLF C:N		0.37	0.36	0.40		0.34	0.22	0.39			0.45	0.64		0.40	0.44	0.64
oLF C:N	0.74			0.84	0.74			0.84	0.86	0.96	0.89	0.94	0.79	0.95		0.95
DF C:N			0.54	0.34			0.53	0.24	0.82			0.52	0.74			0.53
Clay	0.73	0.18	0.20	0.39	0.72	0.23		0.43		0.65		0.81		0.70		0.82
CEC	0.86				0.82				0.79	0.26	0.45					
SSA	0.78	0.75	0.77	0.84			0.62	0.81	0.88		0.92	0.95	0.93	0.57	0.90	0.95
Fe(d-ox)			0.46	0.87	0.07	0.22	0.42	0.77				0.92				0.92
Fe (ox-py)	0.84			0.39	0.90			0.38				0.76	0.98			0.75
Al (ox-py)	0.92		0.48	0.50	0.95		0.39	0.43	0.97			0.89	0.93			0.89
M(ox-py)	0.89			0.12	0.95			0.13	0.99			0.53	0.98			0.52
Fe(py)	0.35			0.82	0.41			0.76	0.49		0.54	0.94			0.59	0.95
Al(py)	0.47		0.63	0.68	0.54		0.58	0.61			0.79	0.93			0.83	0.93
Mpy	0.41		0.31	0.78	0.47		0.27	0.71			0.71	0.95			0.76	0.95

[a]Correlations were conducted separately for each landform position, where each set of correlations included all depths and replicates available for all the variables considered. Here, M = Fe + Al, n = 3 for summit, n = 4 for slope, n = 3 for hollow, and n = 4 for plain. Values presented have $p < 0.05$ (the complete data are given in Text S1). Low R^2 values that are significant at $p < 0.05$ signal existence of data with large variability.

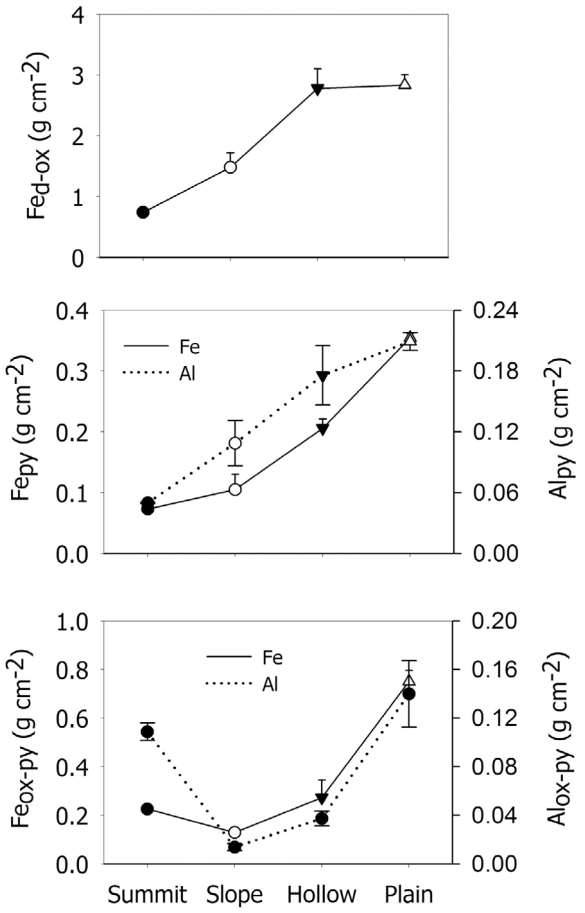

Figure 4. Inventory of metal ions in the eroding and depositional profiles. Bins represent means while error bars represent standard errors for n = 3 in the summit and hollow and for n = 4 in the slope and plain.

positions, but decreased in both depositional positions. However, below 5–15 cm depth, there was a relatively sharp drop in A:O-A ratio with depth for the eroding positions but not the depositional positions (Figure 6). Unlike the eroding slope profiles, and despite the soils' low total C content, the ^{13}C NMR spectra of the hollow at 120–142 cm depth was well resolved and showed particular differentiation into the different functional groups. Although the ^{13}C NMR spectra of the bulk SOM at depth might have been compromised because of the HF treatment, the decrease in A:O-A with depth (especially at the plain site) might not be entirely an artifact of the treatment. *Preston et al.* [1987] observed a similar decrease in A:O-A at depth. The generally observed smaller change in A:O-A ratios and aromaticity for bulk SOM with depth in the depositional profiles, compared to the eroding landform positions (Figure 6), suggests less overall transformation of SOM (i.e., potentially more effective preservation) in the profiles at the depositional positions, compared to the eroding ones.

3.3.3. Density Fractions

[40] To further investigate the above results, we conducted ^{13}C NMR analyses on the density fractions (fLF, oLF and DF) from four depths, at two landform positions with contrasting geomorphology and C content—the slope and the plain (Figure 7). The 10% HF treatment had less impact on the ^{13}C NMR spectra of the dense fraction than it had on the bulk SOM spectra.

[41] Similar to the bulk SOM, for the measured soil layers, important changes in chemical composition of SOM in all three density fractions was observed between the 0–5 and 515 cm depths. The fLF of surface soil at both slope and plain sites had relatively small alkyl peaks, strong O-alkyl signals, small and broad aromatic peaks, and small carboxyl peaks at the surface. With depth, the broad aromatic peak of the fLF became progressively large, and the alkyl peak became more pronounced. At the two bottom layers of the slope and plain profiles, the O-alkyl peak became small and the carboxyl peak gets even smaller and almost disappears.

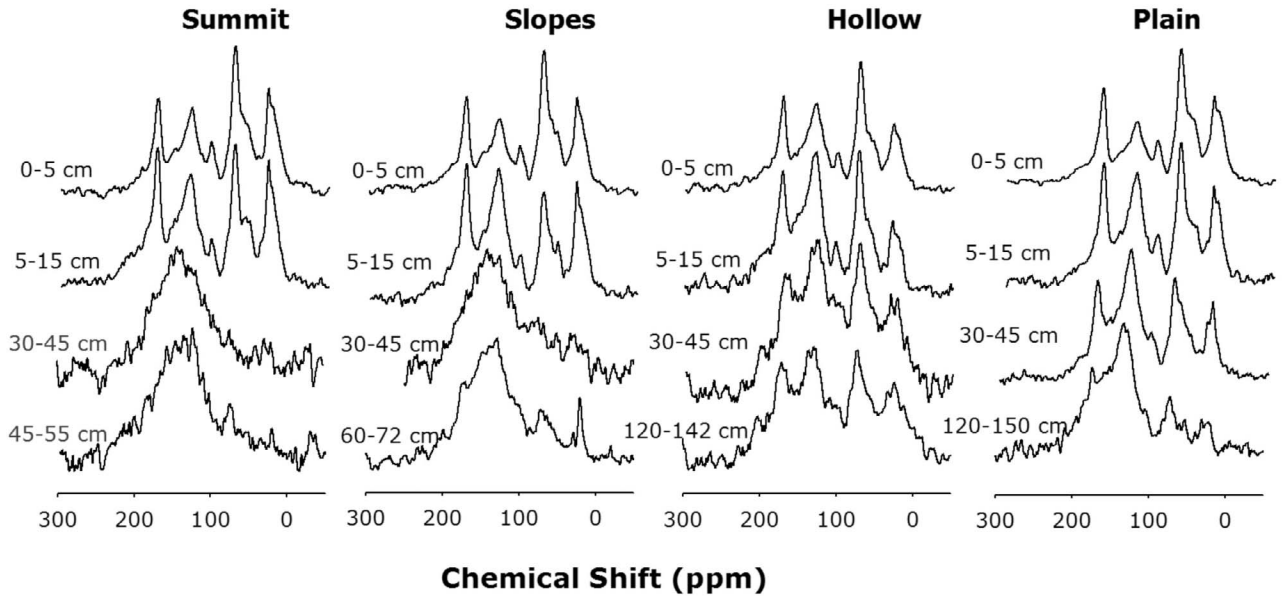

Figure 5. ^{13}C NMR spectra of bulk SOM from the summit, slope, hollow, and plain positions.

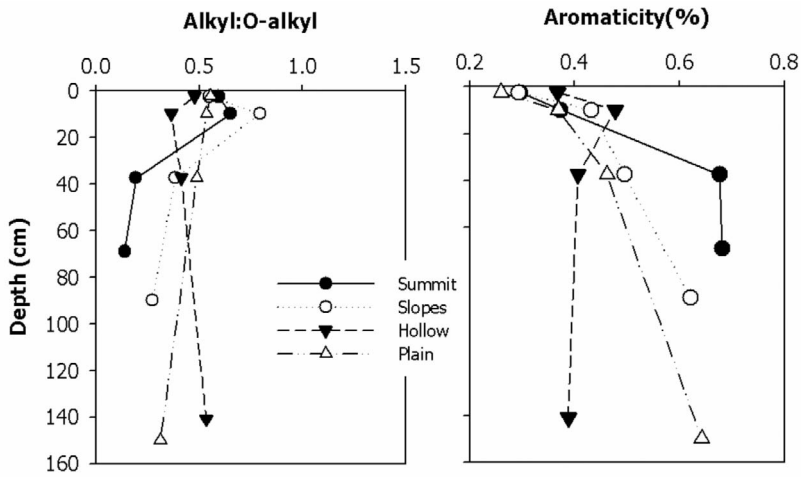

Figure 6. Indices of decomposition (alkyl:O-alkyl) and aromaticity of bulk SOM.

Even at depth, the fLF of both the slope and plain sites had well-resolved alkyl peaks that were not observed in the oLF or DF of either site. In contrast, the alkyl signal of the oLF virtually disappeared from the spectra at depth; the oLF at depth appears to be mainly composed of well-resolved aromatic components. In the DF, however, the alkyl and O-alkyl components had comparable proportions at depth, compared to the near-surface layers, whereas the carboxyl signal intensity was strong (at least until a depth of 45 cm) in both the slope and plain profiles (Figure 7).

[42] The pattern of change in the A:O-A ratio with depth that we observed for the bulk SOM was most closely resembled by the pattern of A:O-A change with depth in the DF of the plain, and to some extent at the slope where A:O-A of the DF ranged from 0.10 to 0.65 at the slope compared to 0.31 to 0.55 at the plain. On average, the greatest difference in A:O-A between slope and plain sites were in the fLF (0.2), compared to bulk SOM and other density fractions (0.01). The widest range in A:O-A for the fLF at the slope indicates that at this eroding position, unprotected SOM exists in a range of decompositional stages. In all cases, the average difference in fraction aromaticity between the slope and the plain profiles is less than 0.1, with the least amount of difference observed in the fLF (0.008) (Figures 7 and 8).

[43] There was a positive correlation between A:O-A ratio and $\Delta^{14}C$ in bulk SOM at both slope and plain sites (R^2 = 0.6 and 0.4, respectively). But among physical fractions, only the DF followed that trend (R^2 = 0.8 in both cases). The A:O-A ratio of fLF was negative correlated with $\Delta^{14}C$ (with R^2 = 0.99 in the slope and 0.94 in the plain), presumably because high input of fresh plant residue would lead to storage of less-decomposed fLF. Whereas for oLF A:O-A is

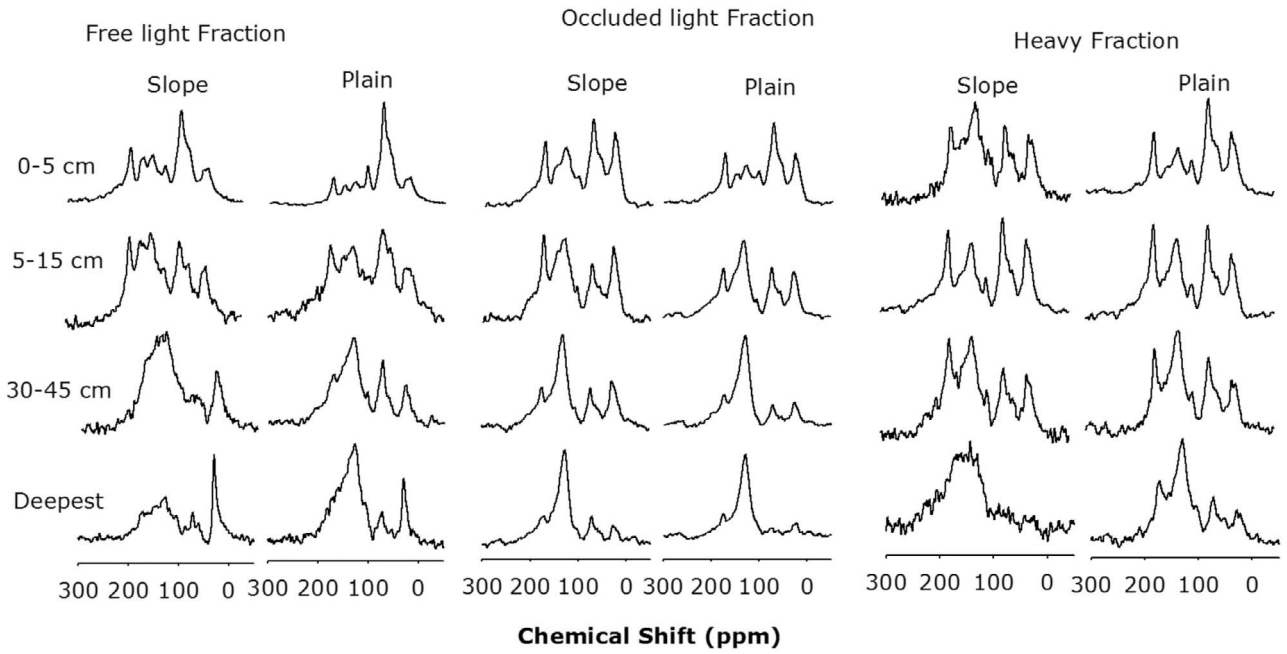

Figure 7. ^{13}C NMR spectra of density fractions from two selected sites: slope and plain.

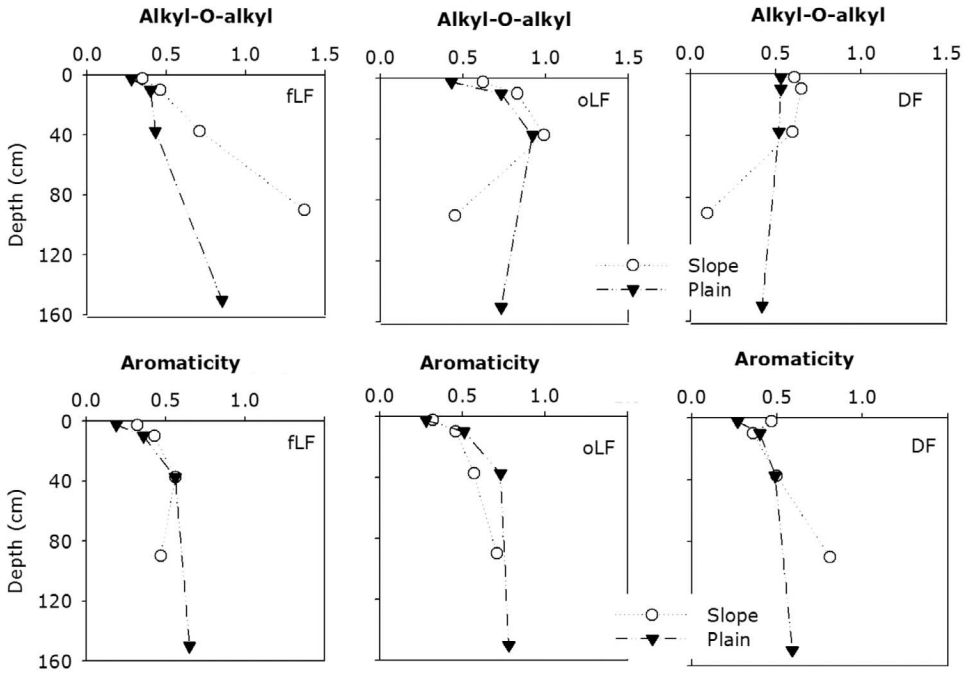

Figure 8. Indices of decomposition (alkyl:O-alkyl ratio) and aromaticity of bulk SOM and all density fractions in the slope and plain. Fraction aromaticity is calculated as [(110 − 160) / (0 − 160)], where 0–45 ppm represents alkyl region, 45–110 ppm represents O-alkyl region, and 110–160 ppm represents aromatic region on the ^{13}C NMR spectra.

directly proportional to $\Delta^{14}C$ in the slope but not in the plain (R^2 = 0.4 in both cases) suggesting that older OM is not necessarily more decomposed, just effectively preserved. Changes in A:O-A and aromaticity with depth were either similar between plain and slope, or lower in plain compared to slope for all fractions we separated. Defining the capacity for preservation of SOM as storage of large amount of old C with small structural modification, the depositional plain exhibited higher capacity for preservation of SOM. This is was especially true for SOM in fLF and DF fractions, more than oLF.

4. Discussion

4.1. Role of Physical Isolation on Persistence of SOM in Eroding and Depositional Landform Positions

[44] Lateral redistribution of SOM due to soil erosion has important implications for not just storage (accumulation) but also stability of SOM in dynamic landscapes. In this study, the preservation of relatively simple, plant-derived molecules (based on NMR spectroscopy) was favored in depositional over erosional landscapes. More C was stored as fLF in the plain, compared to any other landform position indicating that burial of easily assimilable SOM in subsoil of depositional settings is an important mechanism of SOM stabilization.

[45] Profile-averaged ^{14}C (stock-weighted FM; Figure 3) was most depleted in the depositional sites, showing that the ecosystem residence time of C was longer there than in the eroding positions (Figure 4). This may be due in part to the deposition of older material that was fixed in eroding slopes and transported downhill, and the longer MRT of soil particles in depositional compared to eroding landform positions. Radiocarbon was more depleted in the buried soil layers of the poorly drained plain than in the better drained hollow, indicating that the nature of the depositional basin influences whether SOM will be protected from decomposition by burial or not. Consistent with its being a highly dynamic landscape position, the hollow contained the least amount of physically protected SOM (as oLF), and also had OM with lowest C:N ratio of all the landform positions. About 80% of the variability in bulk and mineral-associated C (as DF) stability in the plain could be explained by variability in clay content, while only <2% of the variability in bulk and mineral-associated C stability was attributed to variability in the clay content in the hollow.

[46] In this study we showed that there is no statistically significant difference in the fraction of C that is unprotected (fLF) in the top 40cm of soil at any landform position. Since the stock of active SOM is not higher in the eroding positions than in the depositional positions, it is not likely that there would be massive loss of active C during redistribution as was previously suggested by *Lal* [2003] and *Lal and Pimentel* [2008] especially when the distance traveled by OM from the eroding/source position to the destination/deposition site is short [*Stallard*, 1998a]. In fact, our findings suggest that the combined process of soil erosion and deposition lead to the formation of new aggregates, and may facilitate modification of aggregate size and distribution within the soil providing physical stabilization for eroded SOM in depositional positions. In addition, deposition of eroded SOM in low-lying depositional positions is usually accompanied by reduced oxygen availability and increased soil moisture content in depositional positions, further

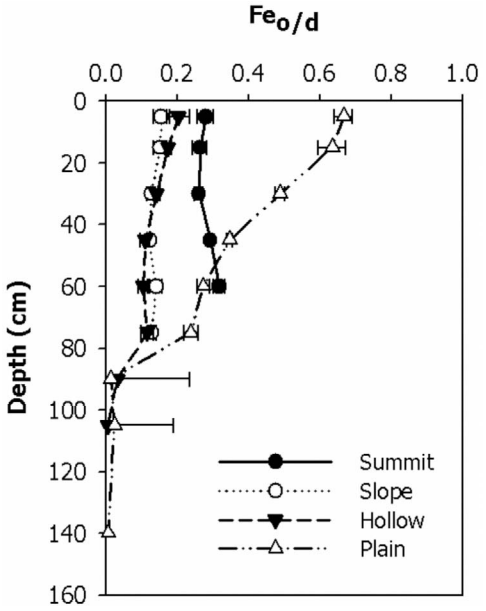

Figure 9. Relative abundance of poorly crystalline versus well-crystallized Fe at the different landform positions.

reducing the rate of OM decomposition [*Sanderman and Amundson*, 2003]. Based on the above findings, we reject hypothesis 1, because more C is not always stored in oLF in depositional landform positions, compared to eroding ones. Our data demonstrate that protection of OM from decay by physical isolation inside aggregates can be effective in poorly drained and clay rich depositional landform positions (such as the plain), but not necessarily in well aerated depositional positions that have low clay content (such as the hollow).

4.2. Role of Interaction With Soil Minerals on Persistence of SOM in Eroding and Depositional Landform Positions

[47] Different chemical associations of OM with the soil mineral fraction were found to be effective in the eroding versus depositional parts of the study watershed. Significant correlation of bulk and mineral-associated C storage with CEC in the summit suggests that interactions with metal cations are likely important mechanisms of C immobilization in this uppermost landform position. The high degree of correlation between OM and CEC is also likely to be a reflection of the high CEC of organic colloids. Crystalline Fe ($Fe_{d\text{-}ox}$) was correlated with both C storage and radiocarbon of bulk and mineral-associated C only in the plain (Table 2). It explains a significant fraction of the variability in C storage but not radiocarbon content in the hollow. In the summit and slope, both bulk and DF radiocarbon content do not show any significant association with $Fe_{d\text{-}ox}$ (except for a week association, $R^2 < 0.22$ between mineral-associated C and $Fe_{d\text{-}ox}$). The lack of or weak association of C and $Fe_{d\text{-}ox}$ in the eroding positions and hollow, respectively, is likely a result of more than 70% of the Fe in these landform positions being found in well-crystallized form (Figure 9). Previous work showed that the two eroding slope positions have reached steady state C storage [*Berhe et al.*, 2008]. These two lines of evidence (weak association of C with $Fe_{d\text{-}ox}$ and steady state C storage) suggest that the eroding positions have maxed out on the ability of Fe oxides to facilitate additional storage and long-term stabilization of SOM by formation of organo-mineral complexes.

[48] Different classes of Fe and Al (oxy)hydroxides were effective for C storage and stabilization at the different landform positions. Due to their small size, oxides when they exist near the soil surface are susceptible to preferential lateral redistribution by soil erosion. In this study, we found that stocks of $Fe_{ox\text{-}py}$ and $Al_{ox\text{-}py}$ explain significant fraction of the variability in bulk and mineral associated C storage and stability in the different soil layers of the summit and plain, which are the landform positions with highest rate of soil production and of deposition of eroded soil, respectively. More than 50% of oxides in the top 50 cm of the soil profile in the plain are made of these poorly crystalline oxide species, compared to 30–40% in the summit, and <20% in the slope and hollow. Although the slope experiences relatively higher rate of soil production compared to the depositional positions [*Yoo*, 2003], it retains the smallest stock of poorly crystalline Fe and Al oxides. It appears that lateral transport of matter from the upper watershed positions (including erosion and seepage) strip the eroding slope profiles of their Fe and Al oxyhydroxides and deposits the oxides downslope in the plain. The high inventory of poorly crystalline Fe and Al oxyhydroxides in the summit (but not slope) suggests a prevalence of preferential transport of fine, poorly crystalline minerals with gopher-facilitated diffusional mass transport only in the steeper sections of the toposequence. In addition, it is possible that lateral and vertical movement of water in the soil system could have significant effects on dispersion of mineral colloids from the eroding soil profiles. Reorganization of the soil's architecture due to redox fluctuations caused by changes in soil water content, and resultant reductive dissolution of Fe (III) to Fe (II) have previously been shown to have important implications for oxide-OM associations [*Berhe et al.*, 2012; *Thompson et al.*, 2006a, 2006b].

[49] Chelation (M_{py} as a proxy), consistently explained significant amount of the variability in bulk and mineral-associated C storage and radiocarbon content in the depositional positions, but not the eroding ones. Complexation was found to be important for C stabilization in all depths below 5 cm in the plain and in the top 70 cm of hollow. Below 80 cm in the hollow, free light or occluded OM fractions were older (most negative $\Delta^{14}C$) indicating stabilization by burial or aggregation. To further investigate this finding, we computed the ratio of $C{:}M_{py}$ to determine whether there is enough stock of Fe and Al ions in the soil for chelation to have a significant influence on C storage in eroding versus depositional landform positions. In this test, following *Oades* [1989] and *Masiello et al.* [2004], we assume each organic C functional group represents six C atoms associated with one negative charge (i.e., the abundance of -COO^- -type carbons in soil organic matter is estimated to be about one out of 6 carbons), and that each of the C atoms is bound to one metal ion in organo-metal complexes with all the metal ions providing one positive countercharge, giving a molar ratio of $C{:}M_{py} = 6$. Accordingly, a $C{:}M_{py}$ ratio 6 > indicates there is not enough stock of M_{py} to bind a significant portion of the SOC, and a $C{:}M_{py}$ ratio < 6 would indicate unused potential for C binding. By considering likely states of OM and Fe and Al ions in soil, complete bonding of all SOC to oxides in this form is likely to happen at $C{:}M_{py}$ of 2–10 [*Masiello et al.*,

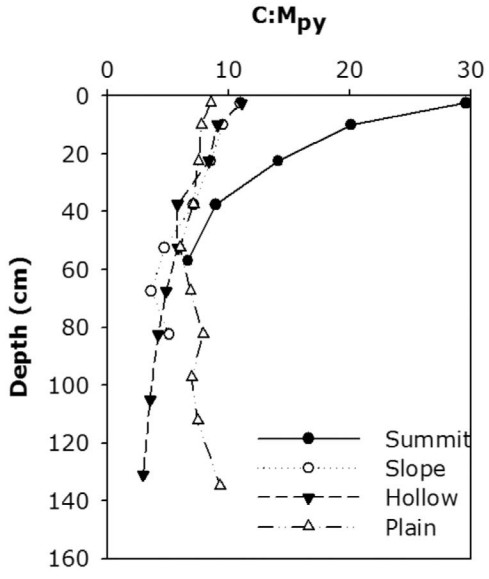

Figure 10. Moles of C per moles of M_{py} (M = Fe + Al).

2004]. For our study, the $C{:}M_{py}$ ratio generally falls within the range of complete bonding, except for the eroding summit position (Figure 10) indicating that chelation is an important mechanism of C stabilization in all landform positions in our study toposequence, except in the summit. At Tennessee Valley, the effectiveness of chelation (M_{py}) as a mechanism of C stabilization decreased as follows: slope ≈ hollow > plain > summit. The stock of Fe_{py} and Al_p in the summit and the plain (Figure 4) is not large enough to chemically stabilize the available SOC in these landform positions by this process alone. Similar to our findings in physical stabilization, the significance of mineral-OM associations for SOM stabilization depend on the nature of the landform position considered. The plain had greater capacity for sorptive stabilization of SOM, compared to the hollow.

[50] The association of OM with soil minerals depends on the nature of the OM. Association of C with Fe oxides was shown to be strongest when C is more processed, at more advanced stages of decomposition where it is likely to be reactive due to accumulation of carboxylic functional groups [*Kleber*, 2005], which may in some cases be characteristic of older OM too. Our findings in this work demonstrate that soil erosion can lead to reconfiguration of chemical, mineral-OM associations by bringing previously unassociated, free OM into contact with unoccupied reactive mineral surfaces, thereby promoting sorptive preservation of eroded and in situ produced OM in depositional positions. Higher stocks of Fe and Al oxides in the hollow and plain, compared to the eroding summit and slope, demonstrate that there is generally higher potential for chemical stabilization of OM in depositional positions than the eroding positions. The linear association of stock and radiocarbon content of SOM (as indicated by the fraction of C in DF and $\Delta^{14}C$ of DF, respectively) with oxides of Fe and Al was not consistently significant (at $p < 0.05$) in the two depositional settings, compared to the eroding ones. In fact, we found that the concentration of oxides explains higher fraction of the variability in SOM storage and radiocarbon content in the summit and plain, compared to the slope and hollow. The higher probability of C to form stabilizing interactions with Fe and Al oxides in the plain but not hollow leads us to reject Hypothesis 2. We conclude that the potential to form new sorptive mineral-organic matter interactions is not always higher in depositional, compared to eroding, landform positions. Protection of OM from decay by chemical association with soil minerals appears to be most effective in poorly drained depositional landform position with high inventory of SOM and oxides, and high rate of OM input from NPP (such as our plain position).

[51] Furthermore, our findings show that Fe oxides may extend the residence time of OM through more ways beyond sorptive interaction with OM fractions [*Berhe et al.*, 2012; *Colombo and Torrent*, 1991; *Denef et al.*, 2002; *Duiker et al.*, 2003] partly due to the small size of oxides and formation of microaggregates and nanoaggregates that can physically protect OM from decomposition and overlap with sorption. Several lines of evidence point to strong role of Fe and Al oxides in formation and stabilization of aggregates in our study site. Despite the fact that the pH in the plain with the highest stock of oxides is not strongly acidic (which would have led to high degree of protonation of the oxide surfaces and consequent biding with OM fractions) we still found that C and Fe are highly correlated and we also see strong association of Fe and Al oxides with stock and radiocarbon content of oLF (Table 3). We found a higher degree of linear association of Fe and Al oxides with biochemical composition and radiocarbon content of physically protected SOM

Table 3. Regression Coefficients (R2 values) Derived From Simple Linear Regression of the Fraction of Physically Protected (oLF) C, C:N of oLf, and Radiocarbon Content of oLF C[a]

	oLF C				oLF C:N				oLF $\Delta^{14}C$			
	Summit	Slope	Hollow	Plain	Summit	Slope	Hollow	Plain	Summit	Slope	Hollow	Plain
Clay								0.90				0.79
CEC					0.77		0.45				0.51	
SSA							0.76				0.90	0.89
Fed-ox	0.42							0.73				0.88
Fepy					0.55	0.27		0.70			0.49	0.96
Alpy			0.28		0.67	0.26		0.58			0.72	0.87
Feox-py					0.66			0.32				0.62
Alox-py					0.87	0.29		0.55	0.97			0.89
Feo/d					0.73			0.83			0.62	0.68

[a]Correlations were conducted separately for each landform position, where each set of correlations included all depths and replicates available for all the variables considered. Here, n = 3 for summit, n = 4 for slope, n = 3 for hollow, and n = 4 for plain ($p < 0.05$). Values presented have $p < 0.05$ (the complete data are given in Text S1). Low R^2 values that are significant at $p < 0.05$ signal existence of data with large variability.

fraction (as indicated by C:N ratio and $\Delta^{14}C$ of oLF) suggesting that Fe and Al oxides play a significant role in physical stabilization of SOM—likely by promoting formation and stabilization of soil aggregates that physically render SOM inaccessible for decomposition. Hence, we conclude that Fe and Al oxides do indeed have stabilizing effects for SOM that extend beyond sorptive interactions of OM fractions with soil minerals. The role of Fe and Al oxides in aggregate formation and stabilization, and its implication for C stabilization was previously confirmed by *Wagai and Mayer* [2007], *von Lützow et al.* [2007] and *Sollins et al.* [1996].

4.3. Contribution of Molecular Structure on Persistence of SOM in Eroding and Depositional Landform Positions

[52] The top 15 cm of the eroding profiles of the summit and slope contain newer SOM (higher FM values, small A:O-A), and weak association of bulk and DF with pyrophosphate extractable Fe and Al. The relatively small change with depth in A:O-A in the depositional profiles compared to the eroding profiles suggest small or no transformation of SOM over the time of deposition, likely because layers of eroded SOM were deposited on top of each other rapidly, leaving little time for decomposition before burial occurred [*Berhe et al.*, 2007]. This conclusion is plausible considering the geomorphic history of the site which includes landslides, diffusive mass transport and exfiltrating surface flows [*Heimsath et al.*, 1997; *Yoo et al.*, 2005, 2006], and considering that the plain site is waterlogged during the rainy season and contains a lot more clay than does the rest of the watershed.

[53] Consistent with the conclusion we reached on density fractions above, the patterns of A:O-A and aromaticity of fLF indicate that deep fLF is more decomposed than fLF near the soil surface. Moreover, subsoil fLF (below 15 cm) was considerably more decomposed in the slope than in the plain possibly because the poor drainage in the plain and successive depositional events result in slower decomposition of eroded C if it is buried in low-lying depositional positions, compared to if it had stayed in the upslope eroding positions. In addition, we find that there is more C protected within mineral aggregates (soil C fraction in oLF) at the plain, compared to the slope. However, at depth, the oLF in the plain profile appears to be younger but more protected against decomposition than the oLF in the slope profile. The large shift in A:O-A at subsurface depth suggests that SOM protected within mineral aggregates undergoes more intense chemical transformation during decomposition near the soil surface in the slope, but once in the subsurface the slope is more efficient in stabilization of oLF than the plain. The finding of eroded C preservation in the depositional positions without significant structural modifications is also corroborated by the trend in our C:N results (Figure 2). Our results of effective stabilization of SOM in deep soil layers is in agreement with recent findings of *Salomé et al.* [2010] where they have shown that OM in deep soil layers persists for longer periods not because it is intrinsically hard to decompose, but rather because accessibility by soil microbes is reduced due to enclosure inside mineral aggregates and deep soil layers. In addition, the accumulation of aromatic SOM at the poorly drained plain, than the relatively well-drained hollow, suggests likely retardation of the activity of obligate aerobic lignin-decomposing fungi and resultant selective preservation of aromatic C associated with lignin [*Baldock et al.*, 1997; *Preston et al.*, 1987].

[54] In our data, we found that the composition of SOM, as indicated by the A:O-A ratio and aromaticity, shows small change with depth in the depositional plain, compared to the eroding slope. Consequently, we accept hypothesis 3 and conclude that the depositional plain favors less OM transformation, more preservation, compared to the slope. It is important to note here that there is no compelling evidence that the process of soil erosion has the potential to separate certain chemical functionalities within OM, leading to selective accumulation of some functional groups. Charcoal is likely the only compound that could be selectively transported by soil erosion, owing to its high porosity, low bulk density compared to denser soil mineral-OM associations [*Hammes et al.*, 2006; *Keiluweit et al.*, 2010]. Soil erosion is not likely to significantly change chemistry of SOM during transport.

5. Conclusion

[55] In this study, we combined different elemental, physical fractionation, and spectroscopic techniques with selective dissolutions to show that very important differences in OM dynamics are likely even within small areas that have the same climate, vegetation assemblages, and parent material. In addition, this study demonstrated how the different techniques can be used in combination to (a) explain dynamics of OM during and after erosion and deposition; (b) explain differences in OM storage across landscapes, and (c) indicate differences in potential vulnerability of SOM in such dynamic landscapes to disturbance. Burial of eroded C in depositional basins can promote C accumulation and extend its residence time within the soil system. However, how much and for how long depositional landform positions may stabilize eroded SOM depends on geomorphology and environmental conditions across the landscape. This study provided evidence that depositional positions may have high fractions of their C stocks in active forms and may be vulnerable to disturbance. Dredging of impoundments or tilling of soil in depositional environments where eroded OM is stored, providing oxygen and access for aerobic decomposition, could release significant amounts of SOC to the atmosphere. Disturbance could take away the physical and chemical mechanisms of SOM protection and fresh, litter-like C could be exposed to decomposition.

[56] Our findings in this study also demonstrate that burial of OM in soil profiles at depositional landform position renders it more stable—as evidenced by the higher storage effectiveness of the depositional positions where SOM underwent relatively small change in molecular composition. Moreover, we demonstrated that processes of soil erosion and deposition may be mechanisms of long-term OM stabilization. We recommend that future studies on soil C cycling should take into account landscape processes rather than exclusively relying on results and models relevant to less dynamic parts of the landscape.

[57] **Acknowledgments.** We wish to thank Corey Lawrence, Elisabet Nadeu, James Kirchner, and Garrison Sposito for their comments on earlier versions of this manuscript; Daniel Keck, Chris Swanston, and Erika Marín-Spiotta for help with density fractionation; and Marjorie Schultz at USGS Menlo Park for guidance during SSA work. The authors also thank two anonymous reviewers and the Associate Editor for their useful comments. This project was supported by National Research Initiative Competitive

Grant 2003-35107-13601 from the USDA Cooperative State Research, Education, and Extension Service, by the USGS Earth Surface Dynamics Program, and by the Office of Science, U.S. Department of Energy, under contract DE-AC02-05CH11231. The ^{13}C NMR work described in this paper was performed in the Environmental Molecular Sciences Laboratory, a national scientific user facility sponsored by the Department of Energy's Office of Biological and Environmental Research and located at Pacific Northwest National Laboratory.

References

Baldock, J. A., J. M. Oades, A. G. Waters, X. Peng, A. M. Vassallo, and M. A. Wilson (1992), Aspects of the chemical structure of soil organic materials as revealed by solid-state ^{13}C NMR spectroscopy, *Biogeochemistry*, *16*(1), 1–42.

Baldock, J. A., J. M. Oades, P. N. Nelson, T. M. Skene, A. Golchin, and P. Clarke (1997), Assessing the extent of decomposition of natural organic materials using solid-state ^{13}C NMR spectroscopy, *Aust. J. Soil Res.*, *35*, 1061–1083, doi:10.1071/S97004.

Berhe, A. A. (2012), Decomposition of organic substrates at eroding vs. depositional landform positions, *Plant Soil*, *350*, 261–280, doi:10.1007/s11104-011-0902-z.

Berhe, A. A., J. Harte, J. W. Harden, and M. S. Torn (2007), The significance of erosion-induced terrestrial carbon sink, *BioScience*, *57*(4), 337–346, doi:10.1641/B570408.

Berhe, A. A., J. W. Harden, M. S. Torn, and J. Harte (2008), Linking soil organic matter dynamics and erosion-induced terrestrial carbon sequestration at different landform positions, *J. Geophys. Res.*, *113*, G04039, doi:10.1029/2008JG000751.

Berhe, A. A., K. B. Suttle, S. D. Burton, and J. F. Banfield (2012), Contingency in the direction and mechanics of soil organic matter responses to increased rainfall, *Plant Soil*, doi:10.1007/s11104-012-1156-0, in press.

Billings, S. A., R. W. Buddemeier, D. deB. Richter, K. Van Oost, and G. Bohling (2010), A simple method for estimating the influence of eroding soil profiles on atmospheric CO_2, *Global Biogeochem. Cycles*, *24*, GB2001, doi:10.1029/2009GB003560.

Blake, G. R., and K. H. Hartge (1986), Bulk density, in *Methods of Soil Analysis: Part 1—Physical and Mineralogical Methods, Agronomy*, vol. 9, 2nd ed., edited by A. Klute, pp. 363–376, Am. Soc. of Agron., Madison, Wis.

Boix-Fayos, C., J. de Vente, J. Albaladejo, and M. Martínez-Mena (2009), Soil carbon erosion and stock as affected by land use changes at the catchment scale in Mediterranean ecosystems, *Agric. Ecosyst. Environ.*, *133*, 75–85, doi:10.1016/j.agee.2009.05.013.

Boudot, J.-P. (1992), Relative efficiency of complexed aluminium, non-crystalline Al hydroxides, allophane and imogolite in retarding the biodegradation of citric acid, *Geoderma*, *52*, 29–39, doi:10.1016/0016-7061(92)90073-G.

Brunauer, S., P. H. Emmett, and E. Teller (1938), Adsorption of gases in multimolecular layers, *J. Am. Chem. Soc.*, *60*, 309–319, doi:10.1021/ja01269a023.

Christensen, B. T. (1992), Physical fractionation of soil and organic matter in primary particle-size and density separates, *Adv. Soil Sci.*, *20*, 1–90, doi:10.1007/978-1-4612-2930-8_1.

Colombo, C., and J. Torrent (1991), Relationships between aggregation and iron oxides in Terra Rossa soils from southern Italy, *Catena*, *18*(1), 51–59, doi:10.1016/0341-8162(91)90006-J.

Denef, K., J. Six, R. Merckx, and K. Paustian (2002), Short-term effects of biological and physical forces on aggregate formation in soils with different clay mineralogy, *Plant Soil*, *246*(2), 185–200, doi:10.1023/A:1020668013524.

Duiker, S., F. Rhoton, J. Torrent, N. Smeck, and R. Lal (2003), Iron (hydr) oxide crystallinity effects on soil aggregation, *Soil Sci. Soc. Am. J.*, *67*(2), 606–611, doi:10.2136/sssaj2003.0606.

Eusterhues, K., C. Rumpel, M. Kleber, and I. Kögel-Knabner (2003), Stabilisation of soil organic matter by interactions with minerals as revealed by mineral dissolution and oxidative degradation, *Org. Geochem.*, *34*, 1591–1600, doi:10.1016/j.orggeochem.2003.08.007.

Golchin, A., J. M. Oades, J. O. Skjemstad, and P. Clarke (1994), Study of free and occluded particulate organic matter in soils by solid state ^{13}C Cp/MAS NMR spectroscopy and scanning electron microscopy, *Aust. J. Soil Res.*, *32*, 285–309, doi:10.1071/SR9940285.

Hammes, K., R. J. Smernik, J. O. Skjemstad, A. Herzog, U. F. Vogt, and M. W. I. Schmidt (2006), Synthesis and characterisation of laboratory-charred grass straw (*Oryza sativa*) and chestnut wood (*Castanea sativa*) as reference materials for black carbon quantification, *Org. Geochem.*, *37*, 1629–1633, doi:10.1016/j.orggeochem.2006.07.003.

Harden, J. W., J. M. Sharpe, W. J. Parton, D. S. Ojima, T. L. Fries, T. G. Huntington, and S. M. Dabney (1999), Dynamic replacement and loss of soil carbon on eroding cropland, *Global Biogeochem. Cycles*, *13*(4), 885–901, doi:10.1029/1999GB900061.

Heimsath, A., W. Dietrich, K. Nishiizumi, and R. Finkel (1997), The soil production function and landscape equilibrium, *Nature*, *388*(6640), 358–361, doi:10.1038/41056.

Heimsath, A., W. Dietrich, K. Nishiizumi, and R. C. Finkle (1999), Cosmogenic nuclides, topography and spatial variation of soil depth, *Geomorphology*, *27*, 151–172, doi:10.1016/S0169-555X(98)00095-6.

Janitzky, P. (1986), Cation exchange capacity, *U.S. Geol. Surv. Bull.*, *1648*, 21–23.

Kahle, M., M. Kleber, and R. Jahn (2002), Predicting carbon content in illitic clay fractions from surface area, cation exchange capacity and dithionite-extractable iron, *Eur. J. Soil Sci.*, *53*, 639–644, doi:10.1046/j.1365-2389.2002.00487.x.

Kaiser, K., and G. Guggenberger (2001), Sorption-desorption of dissolved organic matter in forest soils, paper presented at 11th Annual V. M. Goldshmidt Conference, Lunar and Planet. Inst., Hot Springs, Va.

Keiluweit, M., P. Nico, M. Johnson, and M. Kleber (2010), Dynamic molecular structure of plant biomass-derived black carbon (biochar), *Environ. Sci. Technol.*, *44*, 1247–1253, doi:10.1021/es9031419.

Khosh, M. S., X. Xu, and S. E. Trumbore (2010), Small-mass graphite preparation by sealed tube zinc reduction method for AMS ^{14}C measurements, *Nucl. Instrum. Methods Phys. Res., Sect. B*, *268*(7–8), 927–930, doi:10.1016/j.nimb.2009.10.066.

Kleber, M. (2005), *Mineral Control of Soil Organic Matter Stabilization, Hallenser Bodenwissensch. Abh.*, vol. 8, Der Andere Verlag, Uelvesbüll, Germany.

Kleber, M. (2010a), Response to the opinion paper by Margit von Lützow and Ingrid Kögel-Knabner on "What is recalcitrant soil organic matter?" by Markus Kleber, *Environ. Chem.*, *7*(4), 336, doi:10.1071/EN10086.

Kleber, M. (2010b), What is recalcitrant soil organic matter?, *Environ. Chem.*, *7*(4), 320–332, doi:10.1071/EN10006.

Krull, E. S., J. A. Baldock, and J. O. Skjemstad (2003), Importance of mechanisms and processes of the stabilisation of soil organic matter for modelling carbon turnover, *Funct. Plant Biol.*, *30*(2), 207–222, doi:10.1071/FP02085.

Lal, R. (2003), Soil erosion and the global carbon budget, *Environ. Int.*, *29*(4), 437–450, doi:10.1016/S0160-4120(02)00192-7.

Lal, R., and D. Pimentel (2008), Soil erosion: A carbon sink or source?, *Science*, *319*(5866), 1040–1042, doi:10.1126/science.319.5866.1040.

Loeppert, R. H., and W. P. Inskeep (1996), Iron, in *Methods of Soil Analysis: Part 3—Chemical Methods*, edited by D. L. Sparks et al., *Soil Sci. Soc. Am. Book Ser.*, *5*, 639–664.

Masiello, C. A., O. A. Chadwick, J. Southon, M. S. Torn, and J. W. Harden (2004), Weathering controls on mechanisms of carbon storage in grassland soils, *Global Biogeochem. Cycles*, *18*, GB4023, doi:10.1029/2004GB002219.

Mayer, L. M., and B. S. Xing (2001), Organic matter-surface area relationships in acid soils, *Soil Sci. Soc. Am. J.*, *65*(1), 250–258, doi:10.2136/sssaj2001.651250x.

McCarty, G. W., and J. C. Ritchie (2002), Impact of soil movement on carbon sequestration in agricultural ecosystems, *Environ. Pollut.*, *116*(3), 423–430, doi:10.1016/S0269-7491(01)00219-6.

McKeague, J. A. (1967), An evaluation of 0.1 *M* pyrophosphate and pyrophosphate-dithionite in comparison with oxalate as extractants of accumulation products in podzols and some other soils, *Can. J. Soil Sci.*, *47*, 95–99, doi:10.4141/cjss67-017.

McKeague, J. A., and J. H. Day (1966), Dithionite and oxalate-extractable Fe and Al as aids in differentiating various classes of soils, *Can. J. Soil Sci.*, *46*, 13–22, doi:10.4141/cjss66-003.

Mikutta, R., M. Kleber, M. S. Torn, and R. Jahn (2006), Stabilization of soil organic matter: Association with minerals or chemical recalcitrance?, *Biogeochemistry*, *77*(1), 25–56, doi:10.1007/s10533-005-0712-6.

Nadeu, E., A. A. Berhe, J. de Vente, and C. Boix-Fayos (2011), Erosion, deposition and replacement of soil organic carbon in Mediterranean catchments: A geomorphological, isotopic and land use change approach, *Biogeosciences*, *8*(4), 8351–8382, doi:10.5194/bgd-8-8351-2011.

Oades, J. M. (1988), The retention of organic matter in soils, *Biogeochemistry*, *5*, 35–70, doi:10.1007/BF02180317.

Oades, J. M. (1989), An introduction to organic matter in mineral soils, in *Minerals in Soil Environments*, edited by J. B. Dixon and S. B. Weed, *Soil. Sci. Soc. Am. Book Ser.*, *1*, 89–159.

Oades, J. M. (1995), Recent advances in organomineral interactions: Implications for carbon cycling and soil structure, in *Environmental Impact of Soil Component Interactions*, edited by P. M. Huang et al., pp. 119–134, Lewis, Boca Raton, Fla.

Preston, C. M., S.-E. Shipitalo, R. L. Dudley, C. A. Fyfe, S. P. Mathur, and M. Levesque (1987), Comparison of ^{13}C CPMAS NMR and chemical techniques for measuring the degree of decomposition in virgin and

cultivated peat profiles, *Can. J. Soil Sci.*, *67*, 187–198, doi:10.4141/cjss87-016.

Quine, T. A., and K. Van Oost (2007), Quantifying carbon sequestration as a result of soil erosion and deposition: Retrospective assessment using caesium-137 and carbon inventories, *Global Change Biol.*, *13*(12), 2610–2625, doi:10.1111/j.1365-2486.2007.01457.x.

Rasmussen, C., M. S. Torn, and R. J. Southard (2005), Mineral assemblage and aggregates control carbon dynamics in a California conifer forest, *Soil Sci. Soc. Am. J.*, *69*(6), 1711–1721, doi:10.2136/sssaj2005.0040.

Ross, G. J., and C. Wang (1993), Extractable Al, Fe, Mn and Si, in *Soil Sampling and Methods of Analysis*, edited by M. R. Carter, pp. 239–246, Lewis, Boca Raton, Fla.

Rovira, P., and V. R. Vallejo (2002), Labile and recalcitrant pools of carbon and nitrogen in organic matter decomposing at different depths in soil: An acid hydrolysis approach, *Geoderma*, *107*(1–2), 109–141, doi:10.1016/S0016-7061(01)00143-4.

Salomé, C., N. Nunan, V. Pouteau, T. Z. Lerch, and C. Chenu (2010), Carbon dynamics in topsoil and in subsoil may be controlled by different regulatory mechanisms, *Global Change Biol.*, *16*, 416–426, doi:10.1111/j.1365-2486.2009.01884.x.

Sanderman, J., and R. Amundson (2003), Biogeochemistry of decomposition and detrital processing, *Treatise Geochem.*, *8*, 249–316, doi:10.1016/B0-08-043751-6/08131-7.

Schmidt, M. W. I., and G. Gleixner (2005), Carbon and nitrogen isotope composition of bulk soils, particle-size fractions and organic material after treatment with hydrofluoric acid, *Eur. J. Soil Sci.*, *56*(3), 407–416, doi:10.1111/j.1365-2389.2004.00673.x.

Schmidt, M. W. I., H. Knicker, P. G. Hatcher, and I. Kogel-Knabner (1997), Improvement of ^{13}C and ^{15}N CPMAS NMR spectra of bulk soils, particle size fractions and organic material by treatment with 10% hydrofluoric acid, *Eur. J. Soil Sci.*, *48*, 319–328, doi:10.1111/j.1365-2389.1997.tb00552.x.

Schmidt, M. W. I., et al. (2011), Persistence of soil organic matter as an ecosystem property, *Nature*, *478*, 49–56, doi:10.1038/nature10386.

Sexstone, A. J., N. P. Revsbech, T. B. Parkin, and J. M. Tiedje (1985), Direct measurement of oxygen profiles and denitrification rates in soil aggregates, *Soil Sci. Soc. Am. J.*, *49*, 645–651, doi:10.2136/sssaj1985.03615995004900030024x.

Sheldrick, B. H., and C. Wang (1993), Particle-size distribution, in *Soil Sampling and Methods of Analysis*, edited by M. R. Carter, pp. 499–511, Lewis, Boca Raton, Fla.

Six, J., R. Conant, E. Paul, and K. Paustian (2002), Stabilization mechanisms of soil organic matter: Implications for C-saturation of soils, *Plant Soil*, *241*(2), 155–176, doi:10.1023/A:1016125726789.

Smith, S. V., W. H. Renwick, R. W. Buddemeier, and C. J. Crossland (2001), Budgets of soil erosion and deposition for sediments and sedimentary organic carbon across the conterminous United States, *Global Biogeochem. Cycles*, *15*(3), 697–707, doi:10.1029/2000GB001341.

Sollins, P., P. Homann, and B. A. Caldwell (1996), Stabilization and destabilization of soil organic matter: Mechanisms and controls, *Geoderma*, *74*, 65–105, doi:10.1016/S0016-7061(96)00036-5.

Stallard, R. (1998a), Terrestrial sedimentation and the carbon cycle: Coupling weathering and erosion to carbon burial, *Global Biogeochem. Cycles*, *12*(2), 231–257, doi:10.1029/98GB00741.

Stallard, R. F. (1998b), Terrestrial sedimentation and the carbon cycle: Coupling weathering and erosion to carbon burial, *Global Biogeochem. Cycles*, *12*(2), 231–257, doi:10.1029/98GB00741.

Starr, G. C., R. Lal, J. M. Kimble, and L. Owens (2001), Assessing the impact of erosion on soil organic carbon pools and fluxes, in *Assessment Methods for Soil Carbon*, edited by R. Lal et al., pp. 417–426, Lewis, Boca Raton, Fla.

Staub, B., and C. Rosenzweig (1986), Global Zobler soil type, soil texture, surface slope, and other properties: Digital raster data on a 1-degree geographic (lat./long.) 180 × 360 grid, ftp://ftp.ngdc.noaa.gov/Solid_Earth/cdroms/ged_iia/datasets/a11/sr.htm, Global Ecosystems Database Version 2.0, Natl. Geophys. Data Cent., NOAA, Boulder, Colo. [Updated 1992.]

Stevenson, F. J. (1994), *Humus Chemistry: Genesis, Composition, Reactions*, 496 pp., John Wiley, New York.

Strickland, T. C., and P. Sollins (1987), Improved method for separating light fraction organic material from soil, *Soil Sci. Soc. Am. J.*, *51*, 1390–1393, doi:10.2136/sssaj1987.03615995005100050056x.

Stuiver, M., and H. A. Polach (1977), Reporting of ^{14}C data, *Radiocarbon*, *19*(3), 355–363.

Swanston, C. W., M. S. Torn, P. J. Hanson, J. R. Southon, C. T. Garten, E. M. Hanlon, and L. Ganio (2005), Initial characterization of processes of soil carbon stabilization using forest stand-level radiocarbon enrichment, *Geoderma*, *128*, 52–62, doi:10.1016/j.geoderma.2004.12.015.

Swift, R. S. (1996), Organic matter characterization, in *Methods of Soil Analysis: Part 3—Chemical Methods*, edited by D. L. Sparks et al., *Soil Sci. Soc. Am. Book Ser.*, *5*, 1011–1069.

Tate, K. R. (1992), Assessment, based on a climosequence of soil in tussock grasslands, of soil carbon storage and release in response to global warming, *J. Soil Sci.*, *43*, 697–707, doi:10.1111/j.1365-2389.1992.tb00169.x.

Thompson, A., O. Chadwick, S. Boman, and J. Chorover (2006a), Colloid mobilization during soil iron redox oscillations, *Environ. Sci. Technol.*, *40*, 5743–5749, doi:10.1021/es061203b.

Thompson, A., O. Chadwick, D. Rancourt, and J. Chorover (2006b), Iron-oxide crystallinity increases during soil redox oscillations, *Geochim. Cosmochim. Acta*, *70*(7), 1710–1727, doi:10.1016/j.gca.2005.12.005.

Torn, M. S., S. E. Trumbore, O. A. Chadwick, P. M. Vitousek, and D. M. Hendricks (1997), Mineral control of soil organic carbon storage and turnover, *Nature*, *389*(6647), 170–173, doi:10.1038/38260.

Trumbore, S. (2009), Radiocarbon and soil carbon dynamics, *Annu. Rev. Earth Planet. Sci.*, *37*, 47–66, doi:10.1146/annurev.earth.36.031207.124300.

Trumbore, S. E., J. S. Vogel, and J. R. Southon (1989), AMS ^{14}C measurements of fractionated soil organic matter: An approach to deciphering the soil carbon cycle, *Radiocarbon*, *31*, 644–654.

Van Oost, K., G. Govers, T. Quine, G. Heckrath, J. Olesen, S. De Gryze, and R. Merckx (2005), Landscape-scale modeling of carbon cycling under the impact of soil redistribution: The role of tillage erosion, *Global Biogeochem. Cycles*, *19*(4), GB4014, doi:10.1029/2005GB002471.

Van Oost, K., et al. (2007), The impact of agricultural soil erosion on the global carbon cycle, *Science*, *318*(5850), 626–629, doi:10.1126/science.1145724.

Vogel, J. S. (1992), A rapid method for preparation of biomedical targets for AMS, *Radiocarbon*, *34*, 344–350.

von Lützow, M., I. Kogel-Knabner, K. Ekschmitt, H. Flessa, G. Guggenberger, E. Matzner, and B. Marschner (2007), SOM fractionation methods: Relevance to functional pools and to stabilization mechanisms, *Soil Biol. Biochem.*, *39*(9), 2183–2207, doi:10.1016/j.soilbio.2007.03.007.

Wagai, R., and L. M. Mayer (2007), Sorptive stabilization of organic matter in soils by hydrous iron oxides, *Geochim. Cosmochim. Acta*, *71*(1), 25–35, doi:10.1016/j.gca.2006.08.047.

Xu, X., S. Trumbore, S. Zheng, J. Southon, K. McDuffee, M. Luttgen, and J. Liu (2007), Modifying a sealed tube zinc reduction method for preparation of AMS graphite targets: Reducing background and attaining high precision, *Nucl. Instrum. Methods Phys. Res., Sect. B*, *259*(1), 320–329, doi:10.1016/j.nimb.2007.01.175.

Yoo, K. (2003), Erosion and storage of soil organic carbon in upland hillslope ecosystems, PhD dissertation, 259 pp., Univ. of Calif., Berkeley.

Yoo, K., R. Amundson, A. M. Heimsath, and W. E. Dietrich (2005), Erosion of upland hillslope soil organic carbon: Coupling field measurements with a sediment transport model, *Global Biogeochem. Cycles*, *19*, GB3003, doi:10.1029/2004GB002271.

Yoo, K., R. Amundson, A. Heimsath, and W. Dietrich (2006), Spatial patterns of soil organic carbon on hillslopes: Integrating geomorphic processes and the biological C cycle, *Geoderma*, *130*(1–2), 47–65, doi:10.1016/j.geoderma.2005.01.008.